Nutrient condition in the microenvironment determines essential metabolisms of CD8$^+$ T cells for enhanced IFNγ production by metformin

Chao Ruoyu, Mikako Nishida, Nahoko Yamashita, Miho Tokumasu, Zhao Weiyang, Ikuru Kudo, and Heiichiro Udono

Department of Immunology, Okayama University Graduate School of Medicine, Dentistry, and Pharmaceutical Sciences, Okayama, 700, Japan.

Running title; Metformin's direct effect on CD8$^+$ T cells

Correspondence:

Heiichiro Udono MD. Ph.D.

udono@cc.okayama-u.ac.jp

Keywords: CD8T cells, IFNγ, glycolysis, FAO, autophagy, glutaminolysis,

Abstract

Metformin (Met), a first-line drug for type 2 diabetes, lowers blood glucose levels by suppressing gluconeogenesis in the liver, presumably through the liver kinase B1-dependent activation of AMP-activated protein kinase (AMPK) after inhibiting respiratory chain complex I. Met is also implicated as a drug to be repurposed for cancers; its mechanism is believed identical to that of gluconeogenesis inhibition. However, AMPK activation requires high Met concentrations at more than 1 mM, which are unachievable *in vivo*. The immune-mediated antitumor response might be the case in a low dose Met. Thus, we proposed activating or expanding tumor-infiltrating CD8$^+$ T cells (CD8TILs) in a mouse model by orally administering Met in free drinking water. Here we showed that Met, at around 10 μM and a physiologically relevant concentration, enhanced production of IFNγ,TNFα and expression of CD25 of CD8$^+$ T cells upon TCR stimulation. Under a glucose-rich condition, glycolysis was exclusively involved in enhancing IFNγ production. Under a low-glucose condition, fatty acid oxidation or autophagy-dependent glutaminolysis, or both, was also involved. Moreover, phosphoenolpyruvate carboxykinase 1 (PCK1), converting oxaloacetate to phosphoenolpyruvate, became essential. Importantly, the enhanced IFNγ production was blocked by a mitochondrial ROS scavenger and not by an inhibitor of AMPK. In addition, IFNγ production by CD8TILs relied on pyruvate translocation to the mitochondria and PCK1. Our results revealed a direct effect of Met on IFNγ production of CD8$^+$ T cells that was dependent on differential metabolic pathways and determined by nutrient conditions in the microenvironment. (238 words).

1 Introduction

Cancer incidence and mortality are significantly improved in patients with diabetes who take metformin (Met) for a long period compared with those taking other anti-diabetes drugs (1, 2, 3). As a result, the antineoplastic effect of Met has received increasing attention. However, the precise mechanism of the Met-

dependent antineoplastic effect is highly controversial, according to current research. As respiratory chain complex I is a target of Met (4, 5), the inhibition of oxidative phosphorylation (OxPhos) followed by the activation of liver kinase B1 (LKB1)/ AMP-activated protein kinase (AMPK) axis may downregulate mTORC1 in tumor cells (6,7,8). However, this strategy requires treatment with Met at the mM range, which is practically impossible to achieve in the clinical setting. For example, according to a previous study, Met concentrations in plasma and tumor are both in the range of 3.2 to12.4 μM when the mice receive 1.25 mg/mL Met in free drinking water (9); the dosage of Met is close to that for the patients with diabetes receiving Met. Usually, these concentrations of Met do not inhibit tumor growth *in vitro*.

Previously, we reported that Met administration via free drinking water rendered the mice to reject once established, highly immunogenic solid RL1 tumor (10). This phenomenon was mediated by CD8 T^+ cells as the injection of an anti-CD8 monoclonal antibody (mAb) abolished Met's antitumor effect. A similar effect was observed in other tumor models, such as Renca (renal cell carcinoma), and a smaller effect in four other tumor models (10). Moreover, we recently demonstrated that Met-induced mitochondrial ROS (mtROS) stimulated both Glut-1expression on cell surface of tumor-infiltrating $CD8^+$ T cells (CD8TILs) to produce IFNγ and activation of Nrf2/mTORC1/p62 axis for CD8TILs to proliferate in tumor (11). In another study, Met was shown to enhance the effect of the cancer immunotherapy of PD-1 blockade in the MC38 (colon carcinoma) model; the effect was attributed to the improvement in tumor hypoxia following the OxPhos inhibition in tumor cells by Met (12). However, the authors did not propose a direct effect of Met on CD8TILs. In addition to the immune-modulatory effect of Met, there is evidence for the non-immune-mediated antineoplastic effect by biguanides, including phenformin, in immune-deficient mice (13,14). Indeed, we also observed Met's antitumor effect against osteosarcoma in SCID mice; however, the effect was canceled by the injection of anti-CD11b mAb (15), suggesting the involvement of M1-like macrophages or NK cells but not T lymphocytes in certain tumor cells. Meanwhile, other studies suggest that Met's antineoplastic effect is attributed to the downmodulation of PD-L1 on tumor cells via its degradation in the endoplasmic reticulum (ER) (16,17,18). Lastly, a recent study suggests that Met enhances an antitumor vaccine's effect by reducing the PD-L1 levels on tumor cells (19).

The synthesis of the transporters for Met, such as organic cation transporter 1(OCT-1), is critical for the effect of Met. We recently found that protein expressions of OCT-1 and glucose transporter-1 (Glut-1) were substantially enhanced via the stimulation of TCR using anti-CD3 and anti-CD28 antibodies (Abs), although these genes were much less expressed in unstimulated splenic $CD8^+$ T cells (11). Therefore, it is necessary to investigate whether $CD8^+$ T cell functions, such as IFNγ production, are enhanced by Met at a low concentration. The current study revealed the direct effect of Met at 10 μM on IFNγ production by $CD8^+$ T cells and that the essential metabolism varied under different nutrient conditions in the microenvironment.

2 Results

2.1 Met at 1 mM or higher downregulates oxygen consumption rate (OCR) while upregulates ECAR in tumor cells

First, we explored the dose-response relationship between Met and the metabolism of tumor cells. Murine MO5 (B16 melanoma expressing ovalbumin) and 3LL (lung adenocarcinoma) cells were cultured with various doses of Met at 0–5 mM for 48 h. Then, OCR and ECAR were simultaneously examined using a Seahorse flux Analyzer. Consistent with previous studies, OCR was inhibited by Met at 1 mM or higher in both cell lines (Figure 1A, B, E, and F). Surprisingly, ECAR, indicating glycolysis, was elevated by Met at 1 mM or higher in a dose-dependent manner (Figure 1C, D, G, and H), suggesting an acceleration of the Warburg effect in the progression of oxidative stress due to Met at 1 mM or higher. In any case, physiologically relevant concentration of Met below 100 μM did not affect the metabolic profile of tumor cells.

2.2 Less than 100 μM Met enhances IFNγ production by $CD8^+$ T cells upon TCR stimulation

Next, we examined whether Met affected the IFNγ production by $CD8^+$ T cells upon TCR stimulation. $CD8^+$T cells isolated from mice spleen cells using magnet beads were stimulated with anti-CD3 Ab and

anti-CD28 Ab for 72 to 120 h in the presence of varying doses of Met at 0–5 mM to examine the IFNγ production. At 10 μM, Met markedly enhanced IFNγ production during the 72-, 96-, and 120-h incubations (Figure 2). Although Met at 100 μM also enhanced IFNγ production during the 72- and 96-h incubations, the enhancement declined at 120 h (Figure 2). Importantly, Met at greater than 1 mM completely abolished the IFNγ production by $CD8^+$ T cells such that IFNγ levels were even lower than those in the cells without Met (Figure 2). Similar results were observed on the expression of CD25, an activation marker of T cells, on the cell surface (Figure S1A) and on the production of TNFα (Figure S1B) of $CD8^+$ T cells. The results indicated that Met at 10 μM, a physiologically relevant concentration, could enhance the IFNγ production by $CD8^+$ T cells upon TCR stimulation and that Met at concentrations high enough to downregulate OCR of tumor cells, hampered the IFNγ production of $CD8^+$ T cells.

2.3 Enhanced IFNγ production by Met-treated $CD8^+$ T cells is abolished by a mitochondrial ROS scavenger

Recently, we observed that the enhanced IFNγ production by the CD8TILs in mice treated with Met was completely negated by the co-administration of MitoTEMPO, a mitochondrial ROS (mtROS) scavenger (11). Therefore, we examined the effect of MitoTEMPO on the *in vitro* IFNγ production by $CD8^+$ T cells upon TCR stimulation with 10 μM Met. As expected, the enhanced IFNγ production was reduced by MitoTEMPO to the level of the $CD8^+$ T cells without Met treatment (Figure 3A; upper panel, Figure 3B, C). However, compound C, an inhibitor for AMPK, did not suppress the IFNγ production of $CD8^+$ T cells (Figure 3A; lower panel, Figure 3B, C), suggesting that Met stimulated IFNγ production of $CD8^+$ T cells in a mtROS but not AMPK-dependent manner. It is of note that both MitoTEMPO and compound C had no inhibitory effect on IFNγ production of $CD8^+$ T cells upon TCR stimulation without Met (Figure 3D, E). Concerning mitochondrial biogenesis, we examined the level of PGC1α in the cells. Met at 10μM elevated the PGC1α levels in $CD8^+$ T cells in the 96 but not 72-h incubation (Figure 3F). As we previously found that autophagy was involved in the proliferation of CD8TILs in mice treated with Met (11), we checked the level of LC3B, an autophagy marker, in the $CD8^+$ T cells with or without chloroquine (CQ), a blocker of the degradation of LC3B within autophagosomes. The accumulation of LC3B was evident at 72 h post culture, and its level was more pronounced in the 96-h incubation in the presence of CQ (Figure 3G). These findings, together with our previous findings (11), confirmed that Met stimulated the production of mtROS, IFNγ production, PGC1α expression, and autophagy.

2.4 Differential metabolic pathways required for Met-induced IFNγ production by $CD8^+$ T cells and CD8TIL

Next, we searched for the metabolic pathway utilized for the IFNγ production by the $CD8^+$ T cells *in vitro* and the CD8TILs *ex vivo*. The translation of IFNγ in $CD8^+$ T cells depends on the GAPDH in glycolysis (20), while the transcription of the IFNγ gene depends on phosphoenolpyruvate (PEP) (21), a metabolite in glycolysis that is essential in Ca^{2+} mobilization to promote NFAT translocation into the nucleus before IFNγ synthesis. The contribution of GAPDH to IFNγ production exclusively depends on glucose. However, PEP can be generated from either glucose or oxaloacetate in a PCK1-dependent manner (21). Oxaloacetate, a metabolite in the TCA cycle, may be generated from glucose, fatty acid, and glutamine/glutamate, suggesting that PEP generation, and hence IFNγ production, can depend on glycolysis, fatty acid oxidation (FAO), and glutaminolysis. These three mechanisms can fuel the TCA cycle in a process called anaplerosis.

To identify the metabolic (anaplerotic) pathways involved in IFNγ production, we generated effector $CD8^+$ T cells *in vitro* upon TCR stimulation using Met. We also generated CD8TILs *ex vivo* on day 10 from the mice treated with Met from day 7 after inoculation with MO5 tumor cells. The *in vivo* experiment revealed a significant reduction of MO5 cell growth (Figure 4A). In addition, the metabolic pathways and the inhibition sites likely inhibited by the specific inhibitors were shown (Figure 4B). Thus, we evaluated the IFNγ production by the $CD8^+$ T cells *in vitro* and by the CD8TILs *ex vivo* in the presence of the metabolic inhibitors.

We found that only 2DG (a hexokinase inhibitor) blocked the IFNγ production by $CD8^+$ T cells upon TCR stimulation with Met on day 3 (72 h), and etomoxir (a CPT1 inhibitor blocking FAO) significantly blocked

the IFNγ production by $CD8^+$ T cells on day 4 (96 h) (Figure 4C, D, E), suggesting that on day 3, the $CD8^+$ T cells depended on glycolysis only, while on day 4 they depended on both glycolysis and FAO for IFNγ production. Furthermore, in the case of the CD8TILs, 2DG and MPC1 (blocking pyruvate entry to mitochondria), but not etomoxir, significantly blocked IFNγ production, suggesting that pyruvate generation from glucose and its translocation to the mitochondria are involved in the IFNγ production by CD8TILs. It is of note that IFNγ production by $CD8^+$ T cells upon TCR stimulation without Met was not sensitive to inhibition of etomoxir (Figure 4G, H), which was in contrast to the results of $CD8^+$ T cells with Met (Figure 4E).

We further investigated if autophagy, glutaminolysis, and PCK1-dependent pathways were involved in IFNγ production. On day 3, we found in $CD8^+$ T cells a weak inhibition by 3MPA (PCK1 inhibitor) and no inhibition by BPTES (an inhibitor of GLS blocking the glutamine-to-glutamate conversion) and CQ, suggesting that glutaminolysis and autophagy were not involved in IFNγ production by day 3 in $CD8^+$ T cells (Figure 5A, B). However, profound inhibition by 3MPA and CQ and a weak but significant inhibition by BPTES were observed on day 4 in the $CD8^+$ T cells (Figure 5A, C), suggesting that on day 4, $CD8^+$ T cells depended on the PCK1-dependent PEP production from oxaloacetate and autophagy involving glutaminolysis for IFNγ production. It is of note that IFNγ production by $CD8^+$ T cells upon TCR stimulation without Met was not blocked by 3MPA and CQ (Figure 5E, F), in contrast to the results of $CD8^+$ T cells with Met (Figure 5C). Intriguingly, 3MPA significantly blocked the IFNγ production by CD8TILs (Figure 5A, D). As CQ and BPTES did not block the IFNγ production by CD8TILs, autophagy and glutaminolysis were not involved, unlike the results on the $CD8^+$ T cells on day 4. Together with the results in Figure 4F, CD8TILs appear to depend on both glucose-dependent anaplerosis and PCK1-dependent PEP production from oxaloacetate for IFNγ production.

2.5 Glucose prevents the metabolic switch from glycolysis to FAO for IFNγ production by $CD8^+$ T cells

On day 3, the $CD8^+$ T cells exclusively depended on glycolysis for IFNγ production; in contrast, on day 4, the $CD8^+$ T cells depended on FAO, autophagy, and glutaminolysis in a PCK1-dependent manner. We wondered the differential metabolic requirement between days 3 and 4 $CD8^+$ T cells was due to the difference in glucose concentrations in the culture supernatant. Therefore, we monitored the glucose concentration in the culture supernatant. We detected the glucose concentration at 12 mM on day 0, which declined to 6 mM on day 3 and 3–4 mM on day 4 (Figure 6A). There was no significant difference in the glucose concentration in the supernatant of the cells with or without Met (Figure 6A). Therefore, the glucose concentration at 3–4 mM might be a point where the metabolism of $CD8^+$ T cells switched to FAO for IFNγ production in the presence of Met. If so, glucose supplementation to the culture would keep the IFNγ production exclusively dependent on glycolysis. Thus, we added glucose back to the culture to increase the glucose concentration to 12 mM for the final 24 h on day 4, then IFNγ production was evaluated in the presence of metabolic inhibitors. We found that IFNγ production was decreased by CQ, etomoxir, BPTES, EGCG (an inhibitor of GDH blocking the glutamate-to-αKG conversion), and PCK1 inhibitor; on the other hand, IFNγ production was completely restored by glucose supplementation (Figure 6B-F). These data suggest that glucose is a critical factor for determining the metabolic pathways required for IFNγ production by $CD8^+$ T cells *in vitro*.

3 Discussion

The current study reports for the first time the direct effect of Met on the IFNγ production by $CD8^+$ T cells. OCT1, a transporter for Met, was shown to be significantly enhanced in $CD8^+$ T cells by TCR stimulation *in vitro* (11), suggesting that the direct effect of Met was only on activated T cells and not on naive T cells. This finding is consistent with the *in vivo* observation that Met administration activates IFNγ production of CD8TILs but not $CD8^+$T cells in the lymph node and the spleen (11). The suitable concentration of Met for IFNγ production by $CD8^+$ T cells is less than 100 μM and ideally 10μM, a physiologically relevant concentration. Our findings may contribute to the understanding of Met's antineoplastic effect on patients with diabetes whose plasma concentration of Met is around 10 μM; thus, the effect may be mediated by the immunosurveillance mechanism. Our findings are consistent with another study, which found that the direct effect of 10 μM Met on NK cells to produce IFNγ might be involved in immunosurveillance (22).

Met at 1 mM or higher inhibits oxidative phosphorylation (OxPhos) while stimulating glycolysis of tumor cells. It may imply that Met at 1mM enhances the Warburg effect, which may have a risk to give preferential effect for the tumor to survive under certain conditions, even if such a high concentration of Met was possible *in vivo*.

T cells almost do not produce IFNγ when the glucose concentration is less than 1 mM due to the GAPDH-mediated- inhibition of IFNγ synthesis (20) and the reduced production of PEP, which is essential for the transcription of the IFNγ gene (21). The glucose concentration in our *in vitro* experiments was found to be 3–12 mM, more than sufficient for IFNγ production. However, the metabolic pathways involved are different for 3mM and 12 mM glucose. Thus, $CD8^+$ T cells shift their dependence on glycolysis to FAO or autophagy-dependent glutaminolysis or both, followed by PCK1-dependent IFNγ production, as the glucose concentration declined to 3mM on day 4 from 6mM on day 3. The flexible metabolism of $CD8^+$ T cells is indeed the case in the presence of Met and is not observed without Met. Met-dependent PGC1α synthesis and autophagy induction became apparent after 96 h of incubation, coinciding with the metabolic switch to FAO from glycolysis. Thus, mitochondrial activation by anaplerosis with fatty acids or glutamine/glutamate or both might be a key step for the metabolic reprogramming in $CD8^+$ T cells.

Quite surprisingly, the *ex vivo* IFNγ production by CD8TILs appeared to depend on glycolysis-derived pyruvate that would be converted to oxaloacetate in the TCA cycle, followed by PCK1-dependent IFNγ production (Figure 7). This pathway might activate both glycolysis and OxPhos in CD8TILs, enhancing IFNγ production and causing cell proliferation, respectively. In fact, our previous study identified a novel role of Met in stimulating the production of mtROS. mtROS stimulates glycolysis to produce IFNγ while promoting cell proliferation via the activation of the Nrf2/mTORC1/p62 axis in CD8TILs (11). CD8TILs metabolism may be unique to Met's treatment because Met upregulates Glut-1 level on the surface of the CD8TILs; moreover, it elevates the glucose concentration in a tumor, likely through the downregulation of the glycolysis of tumor cells in an IFNγ-dependent manner (11). However, CD8TILs metabolism was only examined in MO5 melanoma cells in this study; it is necessary to investigate this mechanism in other tumor models.

The conflicting argument that glycolysis and OxPhos are both most important for effector T cells to fight cancer (23-26), may be two sides of the same coin. The effector function, such as IFNγ production of CD8TILs, is heavily dependent on glycolysis. The analysis of CD8TILs for their IFNγ production revealed the importance of glycolysis over OxPhos. On the other hand, OxPhos is more important in effector T cells that will be adoptively transferred to tumor-bearing mice (26, 27) because the transferred T cells must adapt to a new environment, thus requiring elevated OxPhos in the healthy mitochondria. After ensuring survival in tumor tissues, the transferred T cells can proliferate while fighting cancer. In this phase, Oxphos for cell survival and proliferation and glycolysis for T cell function become important.

Similarly, Met's effect on effector T cells may have different aspects. We previously observed that treatment with Met for a short period of approximately 6 h conferred a better migration or expansion ability, or both, on tumor-specific, naive $CD8^+$ T cells in the tumor after their adoptive transfer to tumor-bearing mice, compared with those of the $CD8^+$ T cells without Met treatment. This effect was blocked by the treatment of T cells with compound C before their adoptive transfer (10); thus, this effect might be AMPK-dependent. However, the specificity of compound C is broad beyond AMPK. Met appeared to protect the transferred T cells from apoptosis after their migration into the tumor in this case. The current study, however, has revealed the importance of glycolysis and pyruvate-dependent anaplerosis for IFNγ production by CD8TILs *ex vivo*; the effect is sensitive to MitoTEMPO but not compound C. Concerning the involvement of AMPK for T cell effector function, a previous report suggest that LKB1-AMPK axis negatively regulates T cell function (28), which might be consistent with our results in the current study. Therefore, the AMPK requirements of effector T cells for antitumor response may vary depending on the experimental conditions.

4 Materials and Methods

4.1 Metformin, inhibitors

Metformin hydrochloride (Tokyo Chemical Industry), 2-deoxy-D-glucose (Sigma-Aldrich), Etomoxir (Selleck Chemicals), ethyl sulfide (BPTES, Sigma-Aldrich), Chloroquine hydrochloride (Sigma-Aldrich), UK5099 (Sigma-Aldrich), epigallocatechin gallate (Tokyo Chemical Industry), 3MPA (Sigma-Aldrich), MitoTempo (Sigma-Aldrich), Compound C (Sigma-Aldrich) were purchased.

4.2 Mice

Female C57BL/6 (B6) mice (SLC, Shizuoka, Japan) were used for all experiments. All mice were maintained under specific pathogen-free conditions in the animal facility of Okayama University. This study was approved by The Institutional Animal Care and Use Committee of Okayama University Graduate School of Medicine.

4.3 Tumor cell lines, cell culture

B6 OVA gene-transduced B16 melanoma MO5 cells were used for tumor assays (Eikawa et al., PNAS). Meanwhile, 3LL cells (kindly provided by Dr. H. Yagita at the Juntendo University of Medicine in Tokyo, Japan) were cultured in a 96-well plate with 100 μl of RPMI supplemented with 10% fetal calf serum (FCS), L-glutamine, 2-ME, sodium pyruvate, and NEAA, treated with metformin at 0, 1, 10, 100, 1000, or 5000 μM for 48 h, and used for extracellular flux analysis.

4.4 Extracellular flux analysis

The oxygen consumption rate (OCR) and extracellular acidification rate (ECAR) of MO5 and 3LL cells were measured in XF media (nonbuffered RPMI 1640 containing 10 mM glucose, 2 mM L-glutamine, and 1 mM sodium pyruvate) under basal conditions and in response to mitochondrial inhibitors, 4 μM oligomycin (Sigma-Aldrich), 8μM FCCP (Sigma-Aldrich), or 100 mM 2DG (Sigma-Aldrich) only or 1 μM rotenone (Sigma-Aldrich) combined with 1μM antimycin A (Sigma-Aldrich) and 100 mM 2DG (Sigma-Aldrich) using an XFe96 Extracellular Flux Analyzer (Agilent Technologies). Cell count evaluated for the metabolism were normalized using a Cytation1 Cell Imaging Multi-Mode Reader (BioTek).

4.5 $CD8^+$ T cell purification and expansion

$CD8^+$ T cells were purified from the spleen using magnetic separation (Miltenyi Biotec), cultured with 1μg/ml plate-bound anti-CD3 (eBioscience) and 2 μg/ml soluble anti-CD28 (eBioscience), in a 96-well plate with 200 μl of RPMI supplemented with 10% FCS, 2mM L-glutamine, 5 x 10^{-5}M 2-mercaptoethanol, 1mM sodium pyruvate, and 0.1 mM non-essential amino acids. 5 x 10^4 $CD8^+$ T cells were cultured in each well. Cell blast formation occurred 24 h after cell culture. Cell numbers became 6.5 x 10^5 after 72-hour-culture and dead cells were observed below 10% under microscope by trypsin staining. For the metformin-treated group, cells were treated with metformin at 0, 1, 10, 100, 1000, or 5000 μM. Cells were collected at 48, 96,120 h for extracellular flux analysis or flow cytometry.

4.6 Tumor Engraftment and *in vivo* Metformin treatment

For melanoma cell engraftment, 2×10^5 MO5 cells were suspended in 200 μl of RPMI and injected subcutaneously into the right side of the back of a wild-type C57BL/6 mouse. Then, 7 days after engraftment, 5mg/mL metformin was administered perorally. Next, 3 days after metformin treatment, tumors were collected for FACS analysis. For the tumor volume experiment, the metformin treatment lasted 30 days. The long (a) and short (b) tumor axes were measured using a pair of Vernier calipers to calculate the mean diameter, whereas tumor volume (V) was calculated as $V = ab^2/2$.

4.7 Tumor-infiltrating lymphocytes collection

Tumors were dissected from mice and minced in phosphate-buffered saline (PBS) supplemented with 5 mM EDTA and 2% FCS. Cells were harvested from the minced tumor tissues using the BD Medimachine system. All cells, including TILs and tumor cells, were stained with fluorescently-labeled antibodies (see below) and subjected to flow cytometry.

4.8 Flow Cytometry and intracellular Cytokine staining

For intracellular IFNγ or TNFα measurement, cells were incubated with or without metformin and/or an inhibitor, thus, 2DG (500 mM), Etomoxir (10μM), BPTES (20μM), Chloroquine(50μM), UK5099(10μM), EGCG(50μM), 3MPA(500μM), MitoTempo (50μM), Compound C(10μM), in the presence of 1.25ng/mL Phorbol 12-myristate 13-acetate (PMA, Sigma-Aldrich), 50nM ionomycin (Sigma-Aldrich) and GolgiStop the Protein Transport Inhibitor (containing Monensin, BD Bioscience) for 6 h (Etomoxir only for last 3 h). After incubation, cells were collected for surface staining with CD3 (17A2) and CD8 (53-6.7) Abs in PBS supplemented with 5 mM EDTA and 2% FCS, in the dark for 30min at 4℃, followed by fixation and permeabilization using Fixation/Permeabilization kit (BD Biosciences) in the dark for 30min at 4℃. Then intracellular IFNγ (XMG 1.2) or TNFα (MP6-XT22) Ab probed for cells in the dark for 30min at 4℃. For LC3B measurement, cells were collected for CD8 and CD3 surface staining, LC3B (Novus Biologicals) antibodies staining was performed using a Fixation/Permeabilization kit (BD Biosciences). For PGC1α measurement, cells were collected for CD8 and CD3 surface staining. Staining for transcription factors was performed with a Transcription Factor Buffer Set (BD Pharmingen™) with PGC1α (Novus Biologicals) antibody. For CD25 measurement, cells were collected and performed CD8, CD3 and CD25 (PC61) surface staining in the dark for 30min at 4℃.

4.9 Measurement of Glucose in $CD8^+$ T cells supernatants

Cell culture Supernatants were collected 72, 96, and 120h after culturing $CD8^+$ T cells and diluted 1:20 for analysis. A Glucose Assay Kit-WST (DojinDo Laboratories) was used to measure the glucose concentrations.

4.10 Glucose supplement for T cells

After 72 h $CD8^+$ T cells culture, D-(+)-glucose (Fujifilm Wako Pure Chemical Corporation) in 10μl of PBS was added to medium to achieve 12mM glucose concentration in culture medium, consisting with the concentration at 0 h. Meanwhile, 10 μl of PBS was added to the negative control group. Flow Cytometry and intracellular cytokine staining were performed 24 h after the glucose supplement.

Conflict of Interest

Authors declare no competing interests.

Author Contribution

C.R. performed the experiments and wrote some parts of paper. M.N. designed the all experiments and supervised the experimental procedures. N.Y. maintained the mice used in the experiments. M.N., M.T., Z.W., and I.K., contributed to the extensive discussion throughout the entire experiments and proof reading of the manuscript. H.U. supervised the project, designed the experiments, and wrote the paper.

Funding

This study was supported by grants to H.Udono from JSPS KAKENHI Grant number 18H04033 and 17K19598.

Acknowledgements

We thank Ms. Tachibana in the animal facility of Okayama University for their kind help to maintain and expanding the mice colony to support this study.

References

1. Evans JM, Donnelly LA, Emslie-Smith AM, Alessi DR, Morris AD. Metformin and reduced risk of cancer in diabetic patients. *BMJ* (2005)330:1304-1305. doi: 10.1136/bmj.38415.708634.F7

2. Bodmer M, Meier C, Krähenbühl S, Jick SS, Meier CR. Long-Term Metformin Use Is Associated with Decreased Risk of Breast Cancer. *Diabetes Care* (2010)33(6):1304–1308. doi: 10.2337/dc09-1791

3. Noto H, Goto A, Tsujimoto T, Noda M. Cancer Risk in Diabetic Patients Treated with Metformin: A Systematic Review and Meta-analysis. *PLOS ONE* (2012)7(3):e33411. doi: 10.1371/journal.pone.0033411

4. Wheaton WW, Weinberg SE, Hamanaka RB, Soberanes S, Sullivan LB, Anso E, et al. Metformin inhibits mitochondrial complex I of cancer cells to reduce tumorigenesis. *eLife* (2014)3:e02242. doi: 10.7554/eLife.02242

5. Birsoy K, Possemato R, Lorbeer FK, Bayraktar EC, Thiru P, Yucel B, et al. Metabolic determinants of cancer cell sensitivity to glucose limitation and biguanides. *Nature* (2014)508:108–112. doi: 10.1038/nature13110

6. Huang X, Wullschleger S, Shpiro N, McGuire VA, Sakamoto K, Woods YL, et al. Important role of the LKB1–AMPK pathway in suppressing tumorigenesis in PTEN-deficient mice. *Biochem J* (2008)412(2):211–221. doi: 10.1042/BJ20080557

7. Foretz M, Hébrard S, Leclerc J, Zarrinpashneh E, Soty M, Mithieux G, et al. Metformin inhibits hepatic gluconeogenesis in mice independently of the LKB1/AMPK pathway via a decrease in hepatic energy state. *J Clin Invest* (2010)120(7):2355-2369. doi: 10.1172/JCI40671

8. Faubert B, Boily G, Izreig S, Griss T, Samborska B, Dong Z, et al. AMPK is a negative regulator of the Warburg effect and suppresses tumor growth in vivo. *Cell Metab* (2013)17(1):113-124. doi: 10.1016/j.cmet.2012.12.001

9. Chandel NS, Avizonis D, Reczek CR, Weinberg SE, Menz S, Neuhaus R, et al. Are Metformin Doses Used in Murine Cancer Models Clinically Relevant? *Cell Metab* (2016)23(4):569-70. doi: 10.1016/j.cmet.2016.03.010

10. Eikawa S, Nishida M, Mizukami S, Yamazaki C, Nakayama E, Udono H. Immune-mediated antitumor effect by type 2 diabetes drug, metformin. *Proc Natl Acad Sci USA* (2015)112(6):1809-1814. doi: 10.1073/pnas.1417636112

11. Nishida M, Yamashita N, Ogawa T, Koseki K, Warabi E, Ohue T, et al. Mitochondrial reactive oxygen species trigger metformin-dependent antitumor immunity via activation of Nrf2/mTORC1/p62 axis in tumor-infiltrating CD8T lymphocytes. *J Immunother Cancer* (2021)9(9):e002954. doi: 10.1136/jitc-2021-002954

12. Scharping NE, Menk AV, Whetstone RD, Zeng X, Delgoffe GM. Efficacy of PD-1 Blockade Is Potentiated by Metformin-Induced Reduction of Tumor Hypoxia. *Cancer Immunol Res* (2017)5(1):9-16. doi: 10.1158/2326-6066.CIR-16-0103

13. Pollak MN. Investigating Metformin for Cancer Prevention and Treatment: The End of the Beginning. *Cancer Discov* (2012)2(9):778-790. doi: 10.1158/2159-8290.CD-12-0263

14. Rajeshkumar NV, Yabuuchi S, Pai SG, De Oliveira E, Kamphorst JJ, Rabinowitz JD, et al. Treatment of Pancreatic Cancer Patient–Derived Xenograft Panel with Metabolic Inhibitors Reveals Efficacy of Phenformin. *Clin Cancer Res* (2017)23(18):5639-5647. doi: 10.1158/1078-0432.CCR-17-1115

15. Uehara T, Eikawa S, Nishida M, Kunisada Y, Yoshida A, Fujiwara T, et al. Metformin induces CD11b+-cell-mediated growth inhibition of an osteosarcoma: implications for metabolic reprogramming of myeloid cells and anti-tumor effects. *Int Immuno* (2019)31(4):187–198. doi: 10.1093/intimm/dxy079

16. Cha JH, Yang WH, Xia W, Wei Y, Chan LC, Lim SO, et al. Metformin Promotes Antitumor Immunity via Endoplasmic-Reticulum-Associated Degradation of PD-L1. *Mol Cell* (2018)71(4):606-620.e7. doi: 10.1016/j.molcel.2018.07.030

17. Chung YM, Khan PP, Wang H, Tsai WB, Qiao Y, Yu B, et al. Sensitizing tumors to anti-PD-1 therapy by promoting NK and CD8+ T cells via pharmacological activation of FOXO3. *J Immunother Cancer* (2021)9:e002772. doi: 10.1136/jitc-2021-002772

18. Veeramachaneni R, Yu W, Newton JM, Kemnade JO, Skinner HD, Sikora AG, et al. Metformin generates profound alterations in systemic and tumor immunity with associated antitumor effects. *J Immunother Cancer* (2021)9:e002773. doi: 10.1136/jitc-2021-002773

19. Munoz LE, Huang L, Bommireddy R, Sharma R, Monterroza L, Guin RN, et al. Metformin reduces PD-L1 on tumor cells and enhances the anti-tumor immune response generated by vaccine immunotherapy. *J Immunother Cancer* (2021)9: e002614. doi: 10.1136/jitc-2021-002614

20. Chang CH, Curtis JD, Maggi LB Jr, Faubert B, Villarino AV, O'Sullivan D, et al. Posttranscriptional control of T cell effector function by aerobic glycolysis. *Cell* (2013)153(6):1239-1251. doi: 10.1016/j.cell.2013.05.016

21. Ho PC, Bihuniak JD, Macintyre AN, Staron M, Liu X, Amezquita R, et al. Phosphoenolpyruvate is a metabolic checkpoint of anti-tumor T cell responses. *Cell* (2015)162: 1217-1228. doi: 10.1016/j.cell.2015.08.012

22. Xia W, Qi X, Li M, Wu Y, Sun L, Fan X, et al. Metformin promotes anticancer activity of NK cells in a p38 MAPK dependent manner. *OncoImmunology* (2021)10(1):1995999. doi: 10.1080/2162402X.2021.1995999

23. Zhang Y, Kurupati R, Liu L, Zhou XY, Zhang G, Hudaihed A, et al. Enhancing CD8+ T cell fatty acid catabolism within a metabolically challenging tumor microenvironment increases the efficacy of melanoma immunotherapy. *Cancer Cell* (2017)32(3):377-391 e9. doi: 10.1016/j.ccell.2017.08.004

24. Zhang C, Yue C, Herrmann A, Song J, Egelston C, Wang T, et al. STAT3 activation-induced fatty acid oxidation in CD8+T effector cells is critical for obesity-promoted breast tumor growth. *Cell Metab* (2020)31: 148-161. doi: 10.1016/j.cmet.2019.10.013

25. Chamoto K, Chowdhury PS, Kumar A, Sonomura K, Matsuda F, Fagarasan S, et al. Mitochondrial activation chemicals synergize with surface receptor PD-1 blockade for T cell-dependent antitumor activity. *Proc Natl Acad Sci USA* (2017)114(5):E761-E770. doi: 10.1073/pnas.1620433114

26. Sukumar M, Liu J, Ji Y, Subramanian M, Crompton JG, Yu Z, et al. Inhibiting glycolytic metabolism enhances CD8+ T cell memory and antitumor function. *J Clin Invest* (2013)123(10):4479-4488. doi: 10.1172/JCI69589

27. Crompton JG, Sukumar M, Roychoudhuri R, Clever D, Gros A, Eil RL, et al. Akt inhibition enhances expansion of potent tumor-specific lymphocytes with memory cell characteristics. *Cancer Res* (2015)75(2):296-305. doi: 10.1158/0008-5472.CAN-14-2277

28. MacIver NJ, Blagih J, Saucillo DC, Tonelli L, Griss T, Rathmell JC, et al. The liver kinase B1 is a central regulator of T cell development, activation, and metabolism. *J Immunol* (2011)187: 4187-4198. doi: 10.4049/jimmunol.1100367

5 Figure Legends

Figure 1. Met at 1 mM or higher downregulates oxygen consumption rate (OCR) while upregulates ECAR in tumor cells. MO5 and 3LL cells were cultured in vitro with the indicated concentrations of Met for 48 h before the extracellular flux analysis. (A–D) The metabolic characteristics of the MO5 cells showing (A) OCR, (B) basal OCR, (C) ECAR and (D) basal ECAR levels. (E–H) The metabolic characteristics of the 3LL cells showing (E) OCR, (F) basal OCR, (G) ECAR and (H) basal ECAR levels. The graphs represented Mean ± SEM of the results of three independent experiments. Statistical analysis was performed by unpaired, two-tailed Student's t-test (*P ≤ 0.05; **P ≤ 0.01; ***P ≤ 0.001; ****P ≤ 0.0001; *****P ≤ 0.00001).

Figure 2. Met below 100 μM enhances IFNγ production by $CD8^+$ T cells upon TCR stimulation. Splenic $CD8^+$ T cells were cultured with the indicated concentrations of Met for 72, 96, and 120 h. The resulting cells were stimulated with PMA and ionomycin for 6 h, followed by the staining of intracellular IFNγ. (A) A representative flow cytometry plot showing the IFNγ levels in the $CD8^+$ T cells. (B–D) The graph represents the percentage of the $IFN\gamma^+$ $CD8^+$ T cells at (B) 72 h, (C) 96 h, and (D) 120 h. (E-G) The graph represents the MFI of the $IFN\gamma^+$ $CD8^+$ T cells at (E) 72 h, (F) 96 h, and (G) 120 h. The graphs represent Mean ± SEM of the results of three independent experiments. Statistical analysis was performed by unpaired, two-tailed Student's t-test (*P ≤ 0.05; **P ≤ 0.01; ***P ≤ 0.001; ****P ≤ 0.0001; *****P ≤ 0.00001).

Figure 3. Met-induced enhancement of IFNγ, PGC1α, and LC3B of $CD8^+$ T cells and the effects of inhibitors. Splenic $CD8^+$ T cells were cultured with anti-CD3 and anti-CD28 Abs in the presence or absence of 10 μM Met for 48, 72 or 96 h. (A-E) The resulting cells were stimulated with PMA and ionomycin in the presence or absence of Met and inhibitors as indicated for 6h. (A) A representative flow cytometry plot showing IFNγ levels in the $CD8^+$ T cells treated with or without MitoTempo (upper panels), and Compound C (lower panels). (B-E) The graph represents the MFI of IFNγ levels at (B, D) 72 h and (C, E) 96 h. (F) A representative flow cytometry plot showing PGC1α levels in the $CD8^+$ T cells that were cultured for 72 or 96 h with or without Met. (G) A representative flow cytometry plot showing LC3B levels in the $CD8^+$ T cells that were cultured for 48,72, and 96h with or without treatment by CQ for last 6h. The graphs represent Mean ± SEM of the results of three independent experiments. Statistical analysis was performed by unpaired, two-tailed Student's t-test (*P ≤ 0.05; **P ≤ 0.01; ***P ≤ 0.001; ****P ≤ 0.0001; *****P ≤ 0.00001).

Figure 4. FAO is essential for IFNγ production by $CD8^+$ T cells cultured for 96 but not 72 hours For *in vitro* activated $CD8^+$ T cell preparation, splenic $CD8^+$ T cells were cultured as in Figure 3. For CD8TILs preparation, mice were treated with Met from day 7 post tumor inoculation, and on day 10, tumors were collected for flow cytometry analysis. The *in vitro* activated $CD8^+$ T cells and CD8TIL were stimulated with PMA and ionomycin in the presence or absence of MPC1i (UK5099, a MPC1inhibitor) for 6h, and Etomoxir (Eto) and 2DG for 3h. (A) MO5 tumor growth curve of mice treated with or without Met. (B) The inhibition sites by the specific inhibitors. (C) The levels of IFNγ of *in vitro* activated CD8T cells (72h, 96h) and CD8TIL treated with or without inhibitors as indicated. (D-H) The graph represents the MFI of IFNγ levels *in vitro* activated CD8T at (D, G) 72h, (E, H) 96 h, and CD8TILs (F). The graphs represent the mean ± SEM of the results of three independent experiments. Statistical analysis was performed by unpaired, two-tailed Student's t-test (*P ≤ 0.05; **P ≤ 0.01; ***P ≤ 0.001; ****P ≤ 0.0001; *****P ≤ 0.00001).

Figure 5. Differential metabolisms required for IFNγ production by *in vitro* activated CD8T cells and CD8TILs
The *in vitro* activated $CD8^+$ T cells and CD8TILs were prepared as in Figure 4. The cells were stimulated with PMA and ionomycin in the presence or absence of 3MPA (PCK1i), chloroquine (CQ), and BPTES for 6h. (A) The levels of IFNγ of *in vitro* activated CD8T cells (72h, 96h) and CD8TIL treated with or without inhibitors as indicated. (B-F) The graph represents the MFI of IFNγ levels *in vitro* activated $CD8^+$ T cells at (B, E) 72h, (C, F) 96 h, and CD8TILs (D). The graphs represent the mean ± SEM of the results

of three independent experiments. Statistical analysis was performed by unpaired, two-tailed Student's t-test (*P ≤ 0.05; **P ≤ 0.01; ***P ≤ 0.001; ****P ≤ 0.0001; *****P ≤ 0.00001).

Figure 6. Glucose concentration determines metabolism required for IFNγ production by *in vitro* activated CD8$^+$ T cells

(A) The graphs represent the glucose concentrations in the supernatant of CD8$^+$ T cell cultured with or without Met. (B–F) *In vitro* activated CD8$^+$ T cells at 72h were further incubated with or without supplementation of glucose for additional 24 hours and the resulting cells were treated with PMA and ionomycin in the presence or absence of inhibitors, as indicated in CQ (B), Etomoxir (C), BPTES (D), epigallocatechin gallate (EGCG) (E), and 3MPA(PCL1i) (F). A representative flow cytometry plot showing the *in vitro* IFNγ levels in the CD8$^+$ T cells at 96 h. The graphs represent the mean ± SEM.

Figure 7. Metabolic preference of *in vitro* activated CD8$^+$ T cells and CD8TILs for Met-induced enhancement of IFNγ production

(A) *In vitro* activated CD8$^+$ T cells at 72 h exclusively depends on glycolysis.
(B) *In vitro* activated CD8$^+$ T cells at 96 h depends on FAO, glutaminolysis/autophagy, and PCK1.
(C) CD8TILs depends on anaplerosis from glucose metabolism and PCK1.

Figure 1.

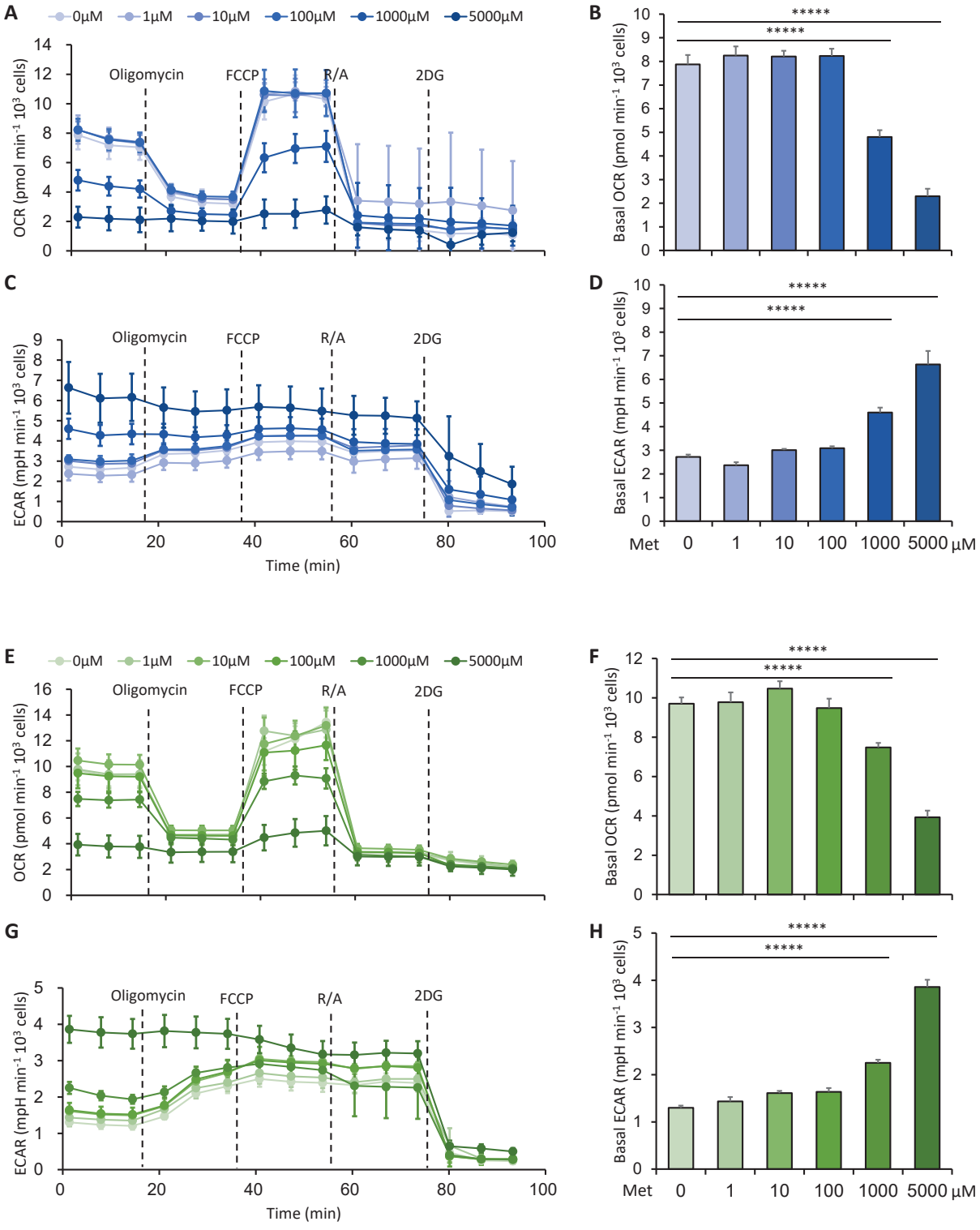
A
0μM
1μM
10μM
100μM
1000μM
5000μM
OCR (pmol min-1 10³ cells)
Oligomycin
FCCP
R/A
2DG
B
Basal OCR (pmol min-1 10³ cells)
*****
C
ECAR (mpH min-1 10³ cells)
Time (min)
D
Basal ECAR (mpH min-1 10³ cells)
Met
0
1
10
100
1000
5000 μM
E
F
G
H

Figure 2.

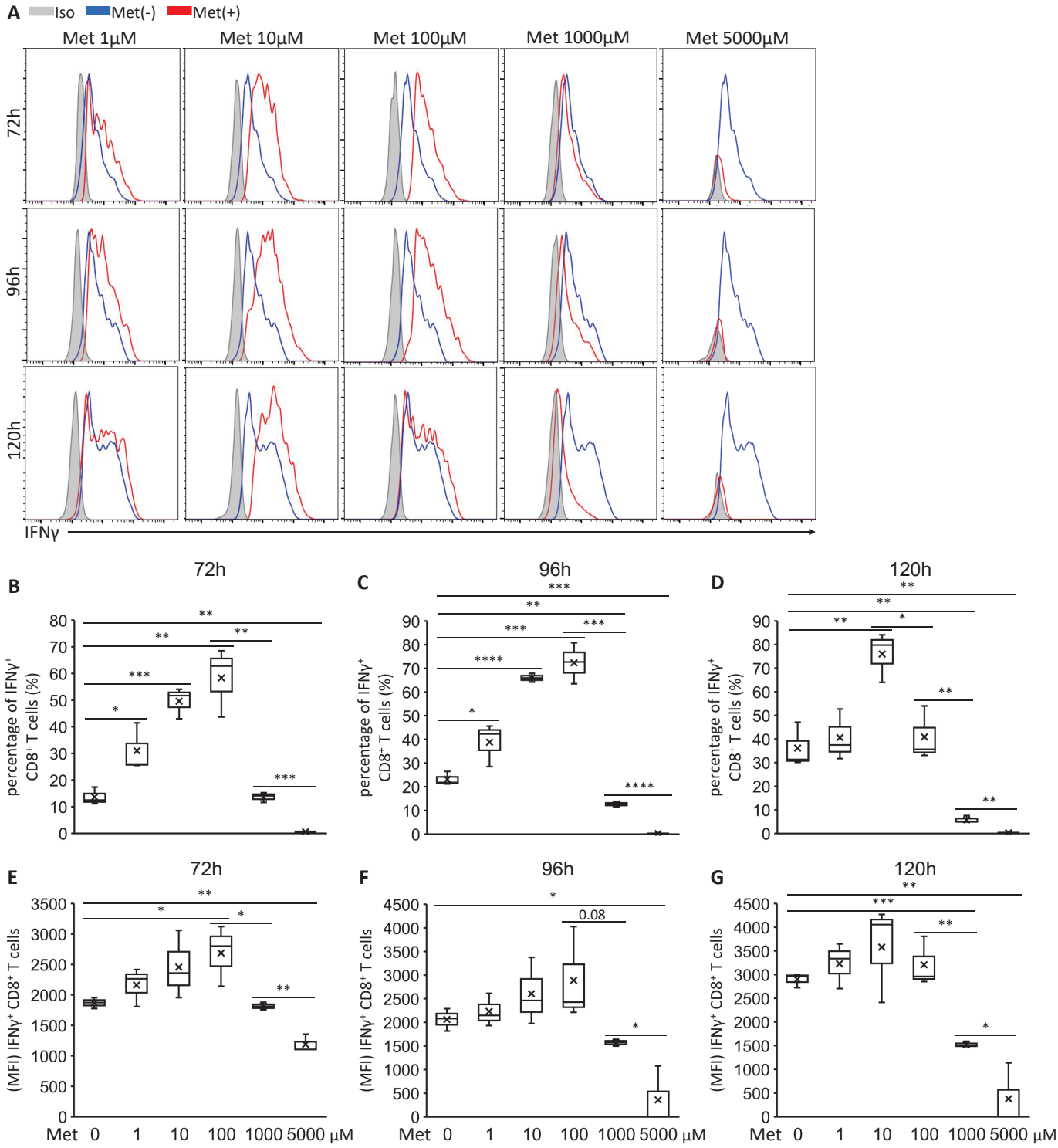
A
Iso
Met(-)
Met(+)
Met 1μM
Met 10μM
Met 100μM
Met 1000μM
Met 5000μM
72h
96h
120h
IFNγ
B
72h
C
96h
D
120h
percentage of IFNγ+ CD8+ T cells (%)
E
72h
F
96h
G
120h
(MFI) IFNγ+ CD8+ T cells
Met 0 1 10 100 1000 5000 μM
0.08

Figure 3.

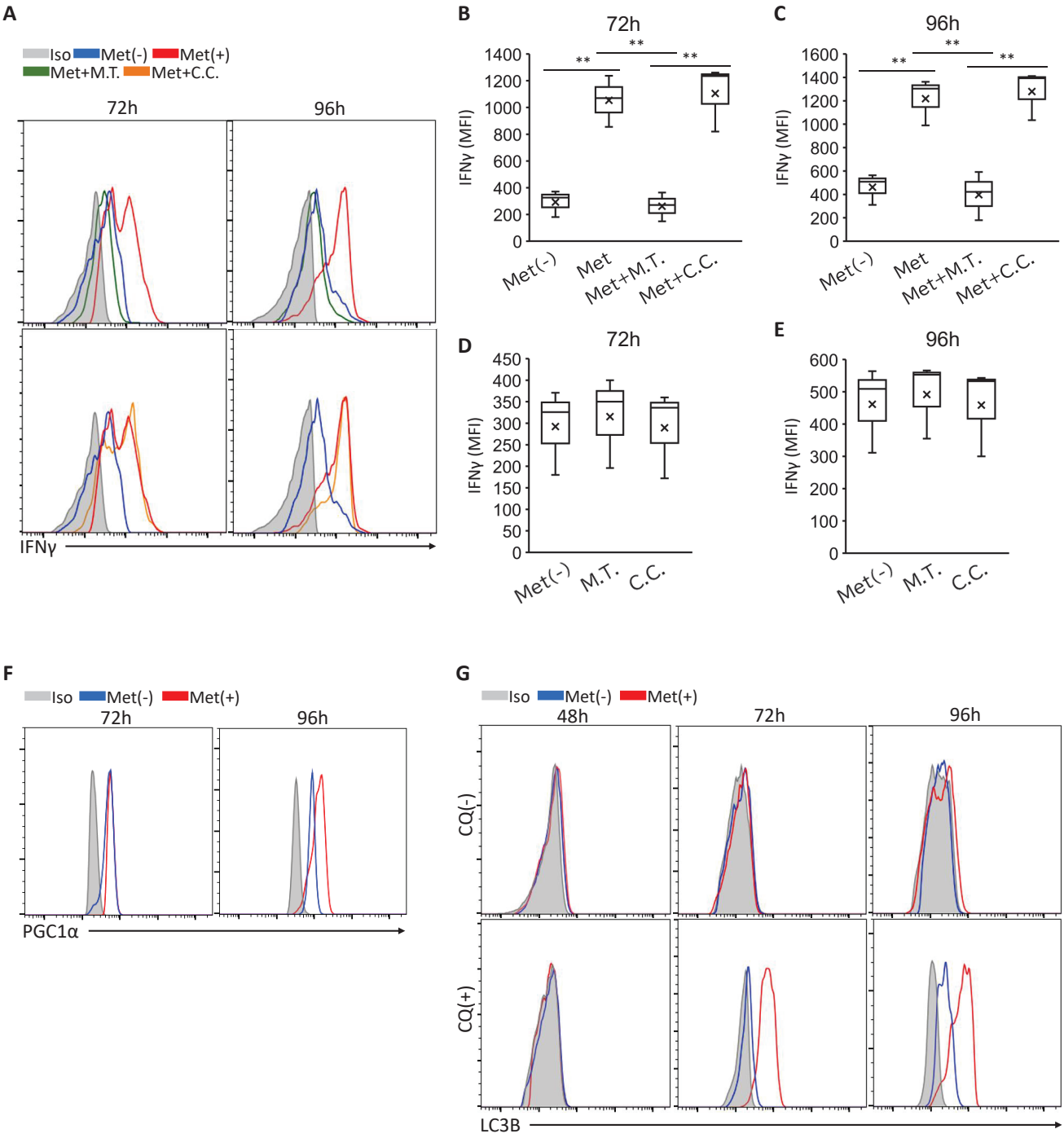
A
Iso Met(-) Met(+)
Met+M.T. Met+C.C.
72h
96h
IFNγ
B
72h
IFNγ (MFI)
Met(-)
Met
Met+M.T.
Met+C.C.
C
96h
IFNγ (MFI)
Met(-)
Met
Met+M.T.
Met+C.C.
D
72h
IFNγ (MFI)
Met(-)
M.T.
C.C.
E
96h
IFNγ (MFI)
Met(-)
M.T.
C.C.
F
Iso Met(-) Met(+)
72h
96h
PGC1α
G
Iso Met(-) Met(+)
48h
72h
96h
CQ(-)
CQ(+)
LC3B

Figure 4.

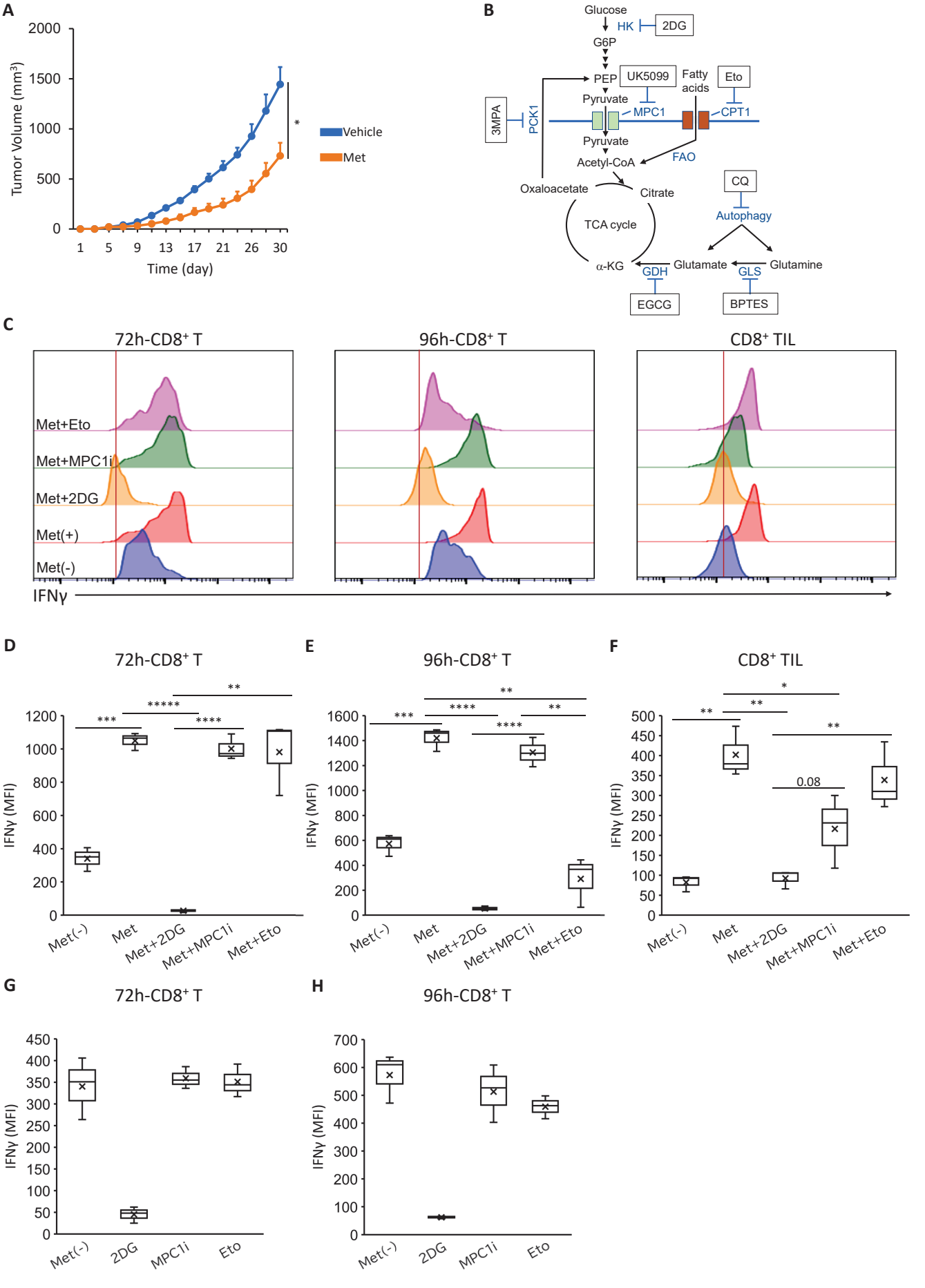
A
Tumor Volume (mm3)
Time (day)
Vehicle
Met
B
Glucose
HK
2DG
G6P
PEP
UK5099
Fatty acids
Eto
Pyruvate
MPC1
CPT1
3MPA
PCK1
Pyruvate
Acetyl-CoA
FAO
Oxaloacetate
Citrate
CQ
Autophagy
TCA cycle
α-KG
Glutamate
Glutamine
GDH
GLS
EGCG
BPTES
C
72h-CD8+ T
96h-CD8+ T
CD8+ TIL
Met+Eto
Met+MPC1i
Met+2DG
Met(+)
Met(-)
IFNγ
D
72h-CD8+ T
E
96h-CD8+ T
F
CD8+ TIL
IFNγ (MFI)
Met(-)
Met
Met+2DG
Met+MPC1i
Met+Eto
0.08
G
72h-CD8+ T
H
96h-CD8+ T
2DG
MPC1i
Eto

Figure 5.

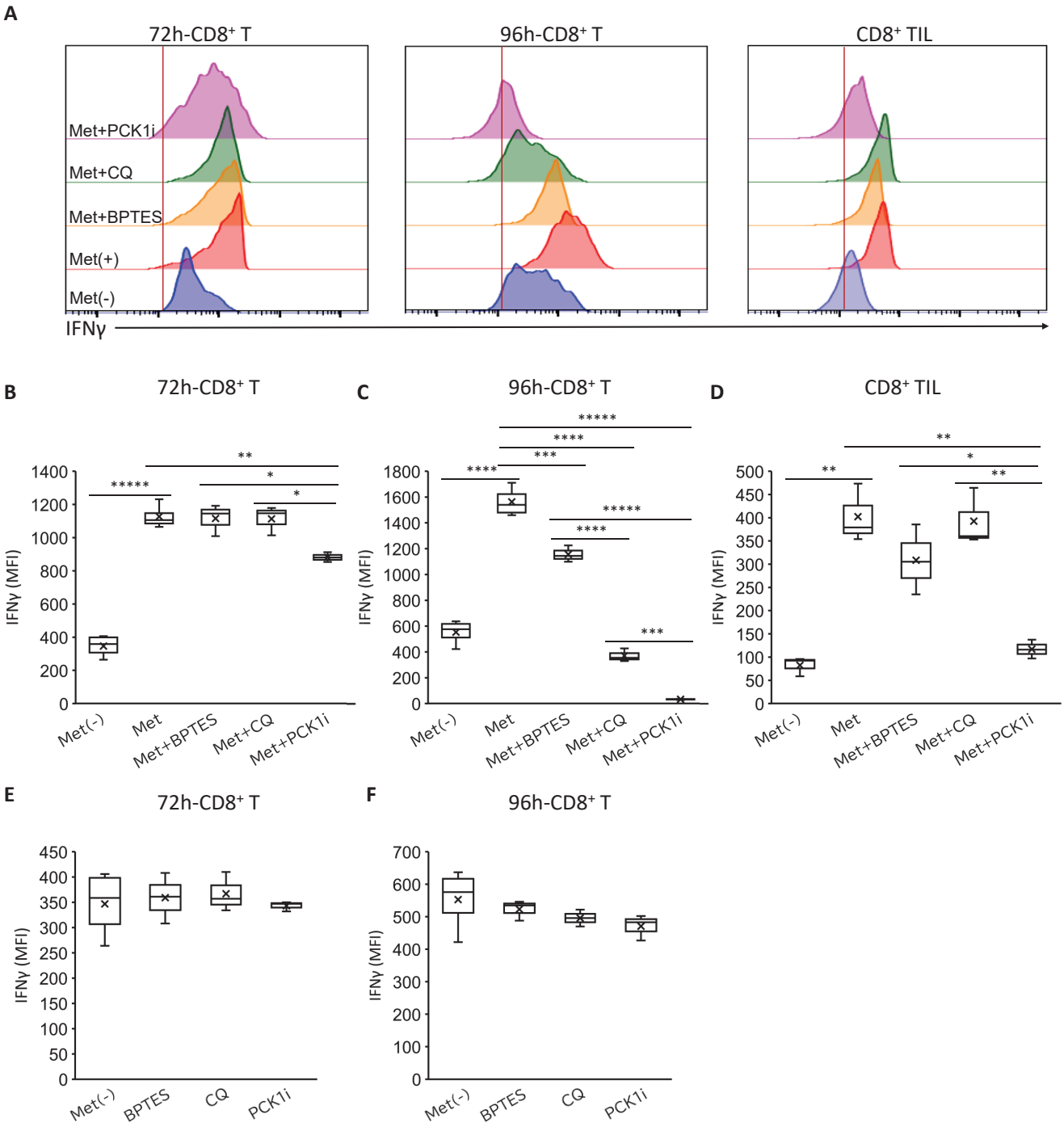
A
72h-CD8⁺ T
96h-CD8⁺ T
CD8⁺ TIL
Met+PCK1i
Met+CQ
Met+BPTES
Met(+)
Met(-)
IFNγ
B
72h-CD8⁺ T
C
96h-CD8⁺ T
D
CD8⁺ TIL
IFNγ (MFI)
Met(-)
Met
Met+BPTES
Met+CQ
Met+PCK1i
E
72h-CD8⁺ T
F
96h-CD8⁺ T
BPTES
CQ
PCK1i

Figure 6.

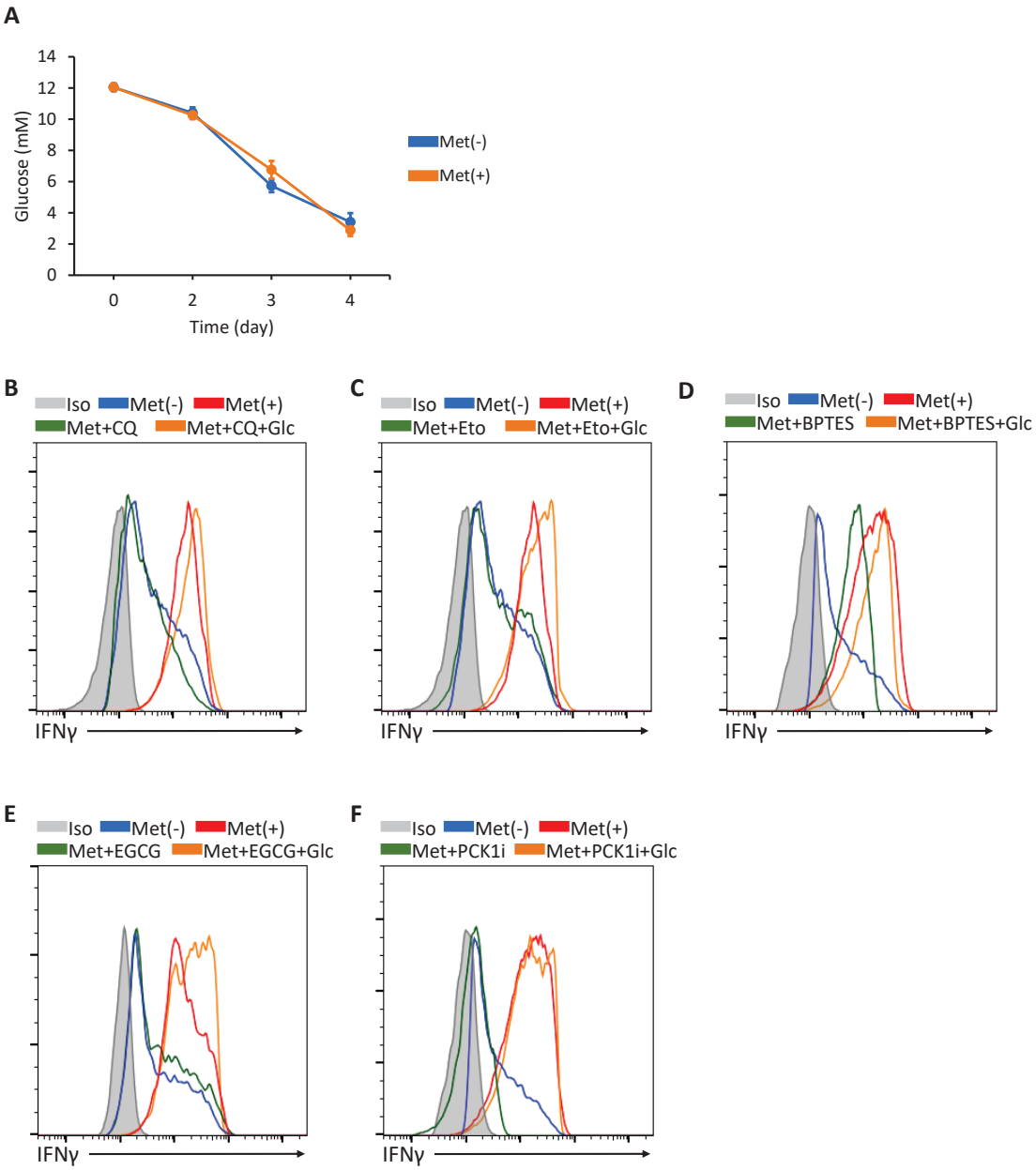
A
Glucose (mM)
Time (day)
Met(-)
Met(+)
B
Iso
Met(-)
Met(+)
Met+CQ
Met+CQ+Glc
IFNγ
C
Met+Eto
Met+Eto+Glc
D
Met+BPTES
Met+BPTES+Glc
E
Met+EGCG
Met+EGCG+Glc
F
Met+PCK1i
Met+PCK1i+Glc

Figure 7.

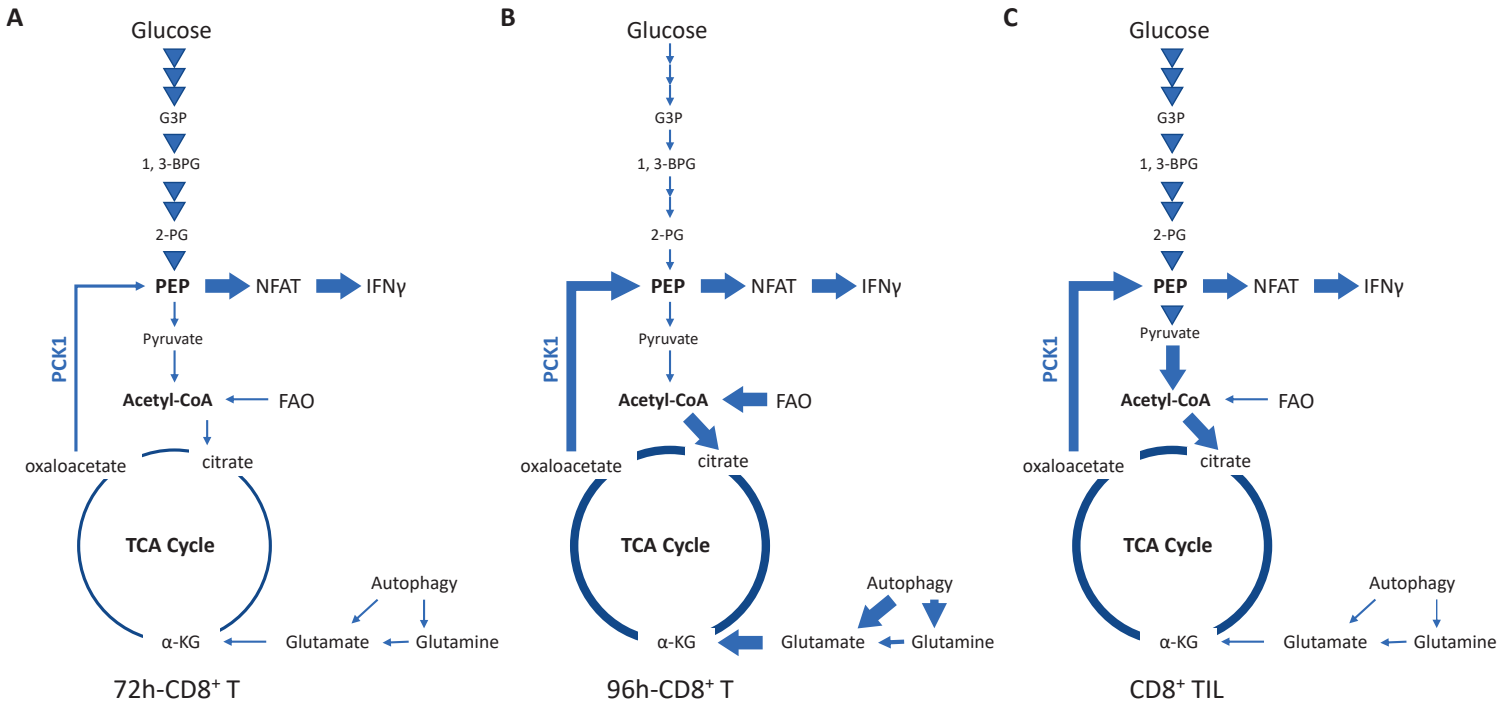
A
Glucose
G3P
1, 3-BPG
2-PG
PEP
NFAT
IFNγ
Pyruvate
PCK1
Acetyl-CoA
FAO
oxaloacetate
citrate
TCA Cycle
Autophagy
α-KG
Glutamate
Glutamine
72h-CD8+ T
B
Glucose
G3P
1, 3-BPG
2-PG
PEP
NFAT
IFNγ
Pyruvate
PCK1
Acetyl-CoA
FAO
oxaloacetate
citrate
TCA Cycle
Autophagy
α-KG
Glutamate
Glutamine
96h-CD8+ T
C
Glucose
G3P
1, 3-BPG
2-PG
PEP
NFAT
IFNγ
Pyruvate
PCK1
Acetyl-CoA
FAO
oxaloacetate
citrate
TCA Cycle
Autophagy
α-KG
Glutamate
Glutamine
CD8+ TIL

Figure S1.

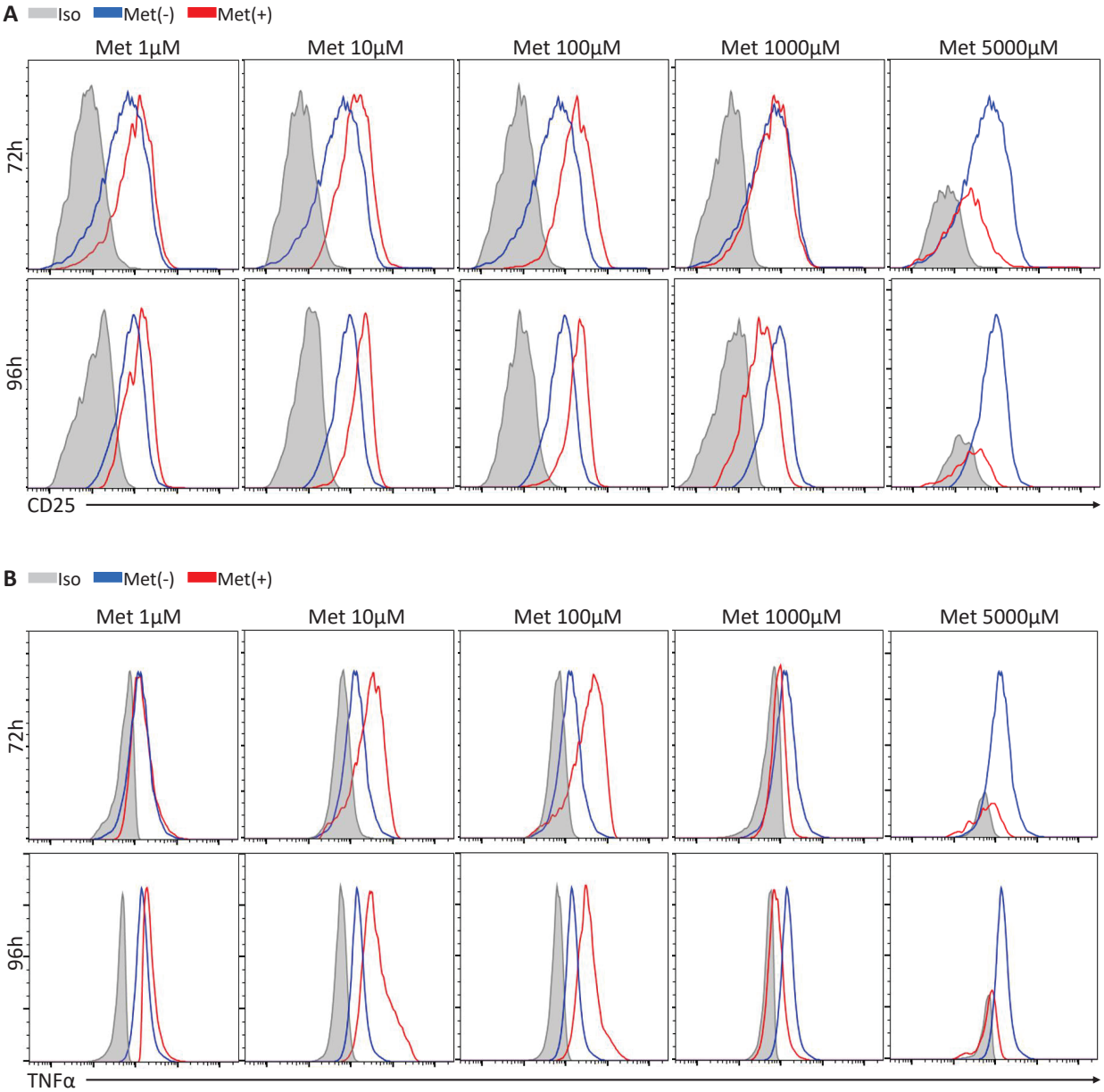

Figure S1. Less than 100 μM Met enhances CD25 expression and TNFα production by CD8$^+$ T cells upon TCR stimulation. Splenic CD8$^+$ T cells were cultured with anti-CD3 and anti-CD28 Abs in the presence or absence of indicated concentrations of Met for 72 or 96 h. (A) A flow cytometry histogram showing CD25 levels on cell surface at 72 h and 96 h. (B) A flow cytometry histogram showing intracellular TNFα levels at 72 h and 96 h.